Harmonic disturbance compensation of a system with long dead-time, design and experimental validation

Can Kutlu Yüksel, Tomáš Vyhlídal, Jaroslav Bušek, Milan Anderle, Silviu-Iulian Niculescu

Harmonic disturbance compensation of a system with long dead-time, design and experimental validation*

Can Kutlu Yüksel, Tomáš Vyhlídal#, Jaroslav Bušek, Milan Anderle, Silviu-Iulian Niculescu

***Abstract*—An internal model control scheme is proposed to compensate both a long dead-time of a system and a harmonic disturbance. The controller is based on an inversion of the first-order model used to approximate the system dynamics together with an input delay. Two other components of the controller consist of a filter and an additional delay by which the harmonic modes are targeted via adjusting the control loop gain and phase shift. The design of the filter-delay pair is fully analytical and the implementation of the scheme is straightforward. The main attention is paid to the complete compensation of a single harmonic disturbance. Besides, an extension of the scheme is proposed to target a double harmonic disturbance. Increased attention is paid to the robustness aspects of the schemes. Outstanding performance in terms of harmonic disturbance compensation of the proposed schemes is demonstrated on a series of laboratory experiments.**

***Index Terms*—Periodic disturbance, internal model, time delay, frequency methods**

I. Introduction

The ability of a system to generate accurate periodic signals is of crucial importance when the system is subjected to such signals either in the form of reference or disturbance. If it is desired to make the system work repetitively, such as for a robotic manipulator, then the system is fed with a periodic reference. On the other hand, if there are rotating or vibrating elements in the working environment, the system may have to execute its task despite the disturbances caused by the environment with periodic characteristics. Regardless of how this periodic signal enters the system, the successful execution of both tasks depends on the ability of the control system to generate a periodic signal.

Arguably, the most common starting point for designing such controllers is the *Internal Model Principle* (IMP). First studied by Francis and Wonham [1], the IMP states that a control system can achieve asymptotic tracking or rejection of an exogenous signal if the closed-loop encompasses a model of the signal (explicitly or implicitly) and is stable.

A particularly popular realization of the Internal Model Principle is the *Repetitive control* which uses a generic *time-delay model* for periodic signals. The inclusion of a generic compensator with a time-delay in the closed-loop brings universal signal coverage; however, introducing a time-delay sub-system with a marginally stable character raises questions about the stability of the resulting control system.

To the best of the authors' knowledge, the first repetitive control design was introduced by Inoue et al. [2] to generate a specific periodic power signal required for the proton synchrotron. The initial stability conditions derived in [2], using the *Small Gain Theorem*, showed that the error stayed bounded for continuous-time proper systems, but did not yield anything for strictly proper systems. Later Hara et al. proved in [3] that the repetitive control system in [2] cannot be exponentially stable for strictly proper systems, and addressed this issue by proposing the modified repetitive control in which a low-pass filter is attached to the time-delay present in the signal model. In parallel, the discrete-time counterpart of the repetitive control was studied by Tomizuka et al. [4], and appropriate conditions for asymptotic convergence were derived.

A high-order repetitive controller design obtained by replacing the time-delay component with an exponential polynomial was proposed in [5]. The weights in the polynomial allowed the controller to be tuned to further improve the non-periodic performance of the repetitive control structure. It was also proven in [6] and [7] that such a modification is also beneficial in improving the robustness of the system to uncertain frequency. Based on the original concepts, the extension of repetitive control to more sophisticated systems has received increasing attention. For instance, some nonlinear applications have been carried out using sliding mode control [8], factorization methods [9], and appropriate passivity properties [10]. Finally, techniques that deal with time-delay systems have been addressed in [11], [12], [13] and [14].

To emphasize the significance of repetitive control, we would like to highlight some of its recent applications, e.g. in electrical stimulation-based wrist tremor suppression [15], nanopositioning stages for high-speed scanning [16], [17], see also [18] for a problem solution with resonant controllers, valve timing control for a digital displacement hydraulic motor [19], see also related problem of harmonic vibration control

*This work was supported by the Czech Science Foundation project No. 21-07321S - *Persistent problems of repetitive control*. The work of the first and fourth authors was also supported by a public grant overseen by the French National research Agency (ANR) as part of the « Investissements d'Avenir » program, through the "ADI 2020" project funded by the IDEX Paris-Saclay, ANR-11-IDEX-0003-02. The first author was also supported by the Grant Agency of the Czech Technical University in Prague, student grant No. SGS23/157/OHK2/3T/12.

T. Vyhlidal (#corresponding author), C.K. Yuksel, J. Busek and M. Anderle are with Dept. of Instrumentation and Control Eng., Faculty of Mechanical Engineering, Czech Technical University in Prague, Technická 1902/4, 166 07 Praha 6, Czech Republic, Tomas.Vyhlidal@fs.cvut.cz

C.K. Yuksel and S.-I. Niculescu are with Université Paris-Saclay, CNRS, CentraleSupélec, Inria, Laboratoire des Signaux et Systèmes, 91192 Gif-sur-Yvette, France, Silviu.Niculescu@l2s.centralesupelec.fr

of cantilever beam [20].

Nevertheless, despite the attention it has received, repetitive control is not the only way to address periodic signals. Alternative realizations of IMP can be carried out through various control schemes and finite-dimensional signal models in contrast to the infinite-dimensional model used by the repetitive control. For instance, a controller for nonlinear systems with finite-dimensional signal model was proposed in [21]. Controllers that employ adaptive finite-dimensional signal models were studied in [22] and [23]. A modified Smith's predictor design for removing periodic disturbance from time-delay systems was discussed in [24]. Methods based on schemes like feed-forward and estimated disturbance-feedback were studied extensively in [25]. A different method was considered by [26], where an observer is proposed to estimate a biased single-harmonic disturbance with an unknown frequency, which is compensated by a nonlinear controller for an electrohydraulic actuator. Finally, in [27], a controller for tracking a multi-harmonic and time-varying periodic signal was proposed.

In this paper, following the preliminary results in [28], we propose and analyze a control scheme which compensates one or two harmonic output disturbances under the presence of *long dead-time*, i.e. dead-time larger than the system time constant. From the point of view of robustness, despite the filter-wise modifications, the repetitive compensator can bring a certain stability risk due to the presence of the modes at or near the stability boundary. The scheme we propose, which is based on the application of Internal Model Control (IMC), directly "targets" one or two modes. Thus, in our opinion, it is much safer. Furthermore, all the delay terms are compensated and the controller design is of finite order nature.

The rest of the paper is organized as follows. Problem motivation and formulation are given in Section II. In Section III, an IMC scheme with a third-order filter to suppress a single harmonic disturbance is presented and analyzed. The preliminary concepts proposed in [28] are supported by extensive analysis and detailed proofs. Increased attention is given to the robustness analysis against mismatch between nominal and true excitation frequency. Additionally, the adjustment of the scheme to suppress a two-mode harmonic signal is included. Thorough experimental validation demonstrating the efficient performance of the proposed schemes can be found in Section IV. A brief summary of the paper and some discussions are given in Section V.

II. Problem formulation

It is commonly accepted that complex dynamics of many industrial processes can be captured by first- or second-order models when combined with delay components [29], [30], [31]. The low-order models essentially capture the dominant time-constant and, if any, dominant oscillatory modes of the complex process. The associated delay then captures all at once the dead-time of the process and the effects of other delay sources like transport or communication. As an example, the hot-rolling mill, which formed the original motivation to develop the controller proposed in this paper, can be approximated by a first-order system with an input delay as discussed in [28], despite the complex dynamics when shaping the material. Likewise, the disturbances these processes are exposed to, when a rotating element is involved within or next to them, have a periodic form with one or two dominant harmonics. For instance, once again in hot rolling mills, the disturbance observed as surface defects are periodic with two dominant harmonics and are caused by the rotating rolls with eccentricities. For reasons stemming from these observations, see e.g. [32] and [33], the paper proposes a controller design for systems that can be approximated by a first-order model with an input time delay of the form:

$$G(s) = \frac{h(s)}{H(s)} = \frac{K}{Ts+1} e^{-\tau_m s}, \tag{1}$$

with time constant T, static gain K and delay τ_m. The resulting delay after approximation can end up being greater than the identified time constant T, implying the need of deliberate handling of the delay. Therefore, the goal of the controller is to compensate for large delays and to suppress the disturbances in the form:

$$d(t) = d_d \sin(\omega_d t + \phi_d) + d_s \sin(\omega_s t + \phi_s) \tag{2}$$

where ω_d, ω_s are target frequencies, d_d, d_s the amplitudes and ϕ_d, ϕ_s phase shifts. At the first stage, a single frequency case is assumed, i.e. $d_s = 0$. Later on, the methodology is extended to the double frequency problem. An experimental validation of our method is proposed in Section IV, in which the mechatronic set-up is designed to mimic the key aspects of plate thickness control under roll eccentricity.

III. Internal model control scheme to attenuate harmonic disturbance

As shown in [34], the *Internal Model Control* (IMC) [35] is a favourable scheme to compensate a long input delay of a system, i.e. the delay τ_m which is longer than the time constant T of the considered model (1). Note that the IMC scheme was studied in [36] to handle the periodic exogenous signals, but without taking into account the input delay. The IMC with a relatively complex filter was validated on the track-following system of an optical disk drive. The proposed modification of

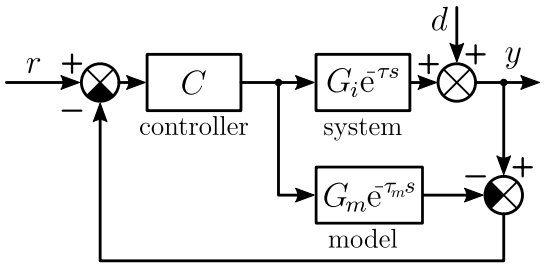

Fig. 1. Internal model control scheme for periodic disturbance compensation, where d, r, y represent disturbance, set-point and controlled output; C is the controller given by (7).

the standard IMC scheme to handle the periodic disturbance, considered first as a single harmonic

$$d(t) = d_d \sin(\omega_d t + \phi_d), \tag{3}$$

is depicted in Fig. 1. The true system dynamics is considered in the form

$$G_p(s) = G_i(s)e^{-s\tau}, \tag{4}$$

where $G_i(s)$ is assumed as non-oscillatory, invertible (i.e. free of non-minimum phase zeros) and possibly of higher order subsystem, and τ is the input delay, representing, e.g., a transportation phenomenon. The system (4) is assumed to be approximated by the model

$$G(s) = G_m(s)e^{-s\tau_m}. \tag{5}$$

Thus, for the considered model (1), we have

$$G_m(s) = \frac{K}{Ts+1}, \tag{6}$$

and τ_m is the overall delay. If $G_i(s)$ is of higher order, then $\tau_m = \tau + \tau_d$ where τ_d approximates the $G_i(s)$ dead-time. In the design and analysis which follows, as well as in the practical applications, it is assumed that the model (4) is not known and only its approximation (5) is available obtained from the process data by a standard identification method [37], [31].

The controller is proposed as

$$C(s) = \frac{e^{-s\vartheta}}{G_m(s)}F(s), \tag{7}$$

where $F(s)$ is a strictly proper filter satisfying

$$\lim_{s\to 0} F(s) = 1. \tag{8}$$

Here, the delay ϑ is included for the purpose of harmonic disturbance compensation. Notice that it is convenient to use the approximate model (1) as it results in a low-complexity controller (7) with the order determined by the filter order.

The *sensitivity function* of the IMC scheme with (7) in Fig. 1 is given by

$$S(s) = \frac{y(s)}{d(s)} = \frac{1 - \frac{1}{G_m(s)}F(s)G_m(s)e^{-s(\tau_m+\vartheta)}}{1 + \frac{1}{G_m(s)}F(s)\left(G_i(s)e^{-s(\tau+\vartheta)} - G_m(s)e^{-s(\tau_m+\vartheta)}\right)}, \tag{9}$$

while the *complementary sensitivity function* is given by

$$T(s) = \frac{y(s)}{r(s)} = \frac{\frac{1}{G_m(s)}F(s)G_i(s)e^{-s(\tau+\vartheta)}}{1 + \frac{1}{G_m(s)}F(s)\left(G_i(s)e^{-s(\tau+\vartheta)} - G_m(s)e^{-s(\tau_m+\vartheta)}\right)}. \tag{10}$$

For the design purposes, assume that the model $G_m(s)$ and system $G_i(s)$ transfer functions are identical and $\tau_m = \tau$ in the nominal form with the controller $C(s)$ given by (7). Then, the sensitivity functions can be simplified to

$$S(s) = 1 - F(s)e^{-s(\tau_m+\vartheta)}, \tag{11}$$

$$T(s) = F(s)e^{-s(\tau_m+\vartheta)}. \tag{12}$$

A. Filter design

The design goal is to find a suitable IMC controller such that it enables the system with long dead-time to asymptotically track the reference r while $\frac{2\pi}{\omega_d}$-periodic signal $d(t)$ acts on the plant's output as the external disturbance. Taking into consideration the nominal form of the sensitivity function (11), the filter should satisfy the following conditions:

Proposition 1: A filter $F(s)$ and the delay ϑ satisfying the following properties

$$|F(j\omega_d)| = 1, \tag{13}$$

$$\arg F(j\omega_d) < 0, \tag{14}$$

$$\vartheta = \frac{2l\pi + \arg F(j\omega_d)}{\omega_d} - \tau_m, \tag{15}$$

with

$$l = \left\lfloor \frac{\tau_m\omega_d - \arg F(j\omega_d)}{2\pi} \right\rfloor + 1 \tag{16}$$

lead to a complete compensation of the harmonic disturbance (3) of the frequency ω_d.

Proof. The total cancellation of the harmonic disturbance (3) with frequency ω_d leads to the condition

$$1 - F(j\omega_d)e^{-j\omega_d(\tau_m+\vartheta)} = 0, \tag{17}$$

which can be turned to

$$1 - |F(j\omega_d)|e^{\arg F(j\omega_d) - j\omega_d(\tau_m+\vartheta)} = 0. \tag{18}$$

This equality requires that (13) should hold simultaneously with

$$\arg F(j\omega_d) - \omega_d(\tau_m + \vartheta) = 2k\pi, k = 0, 1, 3..., \tag{19}$$

from which (15) is derived. Assuming (14), the selection of l by (16) implies the smallest possible delay ϑ. □

In what follows, we propose a low-complexity filter with a structure that is both easy to read and practical to implement. The key benefit is also in its *fully analytic* parameterization.

Proposition 2: The filter in the form

$$F(s) = \bar{F}(s)\tilde{F}(s), \tag{20}$$

with

$$\bar{F}(s) = \frac{\alpha T_f s + 1}{T_f s + 1}, \tag{21}$$

$$\tilde{F}(s) = \frac{\Omega^2}{s^2 + 2\xi\Omega s + \Omega^2}, \tag{22}$$

where the gain $0 < \alpha < 1$ and time constant

$$T_f > \frac{\alpha^{\frac{1}{\alpha-1}}}{\omega_d} \tag{23}$$

are adjustable parameters, fulfills the conditions (13) and (14), by setting

$$\xi = \sqrt{\frac{1 - T_f\omega_d\sqrt{\frac{1-\alpha^2}{T_f^2\omega_d^2+1}}}{2}}, \tag{24}$$

$$\Omega = \frac{\omega_d}{\sqrt{1-2\xi^2}}. \tag{25}$$

Proof. The magnitude of the filter (21) is given by:

$$|\bar{F}(j\omega)| = \sqrt{\frac{\alpha^2 T_f^2 \omega^2 + 1}{T_f^2 \omega^2 + 1}}. \tag{26}$$

Since $0 < \alpha < 1$, (26) is a decreasing function with a limit

$$\lim_{\omega \to \infty} |\bar{F}(j\omega)| = \alpha. \tag{27}$$

The filter also satisfies $\lim_{\omega \to 0} |\bar{F}(j\omega)| = 1$. In Fig. 2, other important points of (26) in logarithmic scale are shown, see the Appendix for the outline of their derivation. The inflection point is at

$$P_I = \left[\frac{1}{T_f \sqrt{\alpha}}, \sqrt{\alpha} \right]. \tag{28}$$

Note that the tangent of the response at this point is independent of T_f and it is given as $\frac{\alpha - 1}{\alpha + 1}$. The breaking points are determined as

$$P_L = \left[\frac{1}{T_f \alpha^{\frac{\alpha}{\alpha - 1}}}, 1 \right], \; P_R = \left[\frac{\alpha^{\frac{1}{\alpha - 1}}}{T_f}, \alpha \right]. \tag{29}$$

The inequality (23) implies that the point P_R is located to the left of ω_d.

The magnitude of filter (22), also satisfying $\lim_{\omega \to 0} |\tilde{F}(j\omega)| = 1$, is given by:

$$|\tilde{F}(j\omega)| = \frac{\Omega^2}{\sqrt{(\Omega^2 - \omega^2)^2 + 4\xi^2 \Omega^2 \omega^2}}. \tag{30}$$

Consider $0 < \xi < \frac{1}{\sqrt{2}}$. Then the magnitude maximum intentionally placed at the target frequency ω_d, which results to (25), satisfies $|\tilde{F}(j\omega_d)| > 1$ and takes place at the point

$$P_M = \left[\omega_d, \frac{1}{2\xi \sqrt{1 - \xi^2}} \right]. \tag{31}$$

Thus, the target condition (13), shown in Fig. 2 at point $P_A = [\omega_d, 1]$, leads to

$$\frac{1}{2\xi \sqrt{1 - \xi^2}} \left| \bar{F}(j\omega_d) \right| = 1. \tag{32}$$

Equation (32) can be expressed as:

$$4\xi^4 - 4\xi^2 + \left| \bar{F}(j\omega_d) \right|^2 = 0, \tag{33}$$

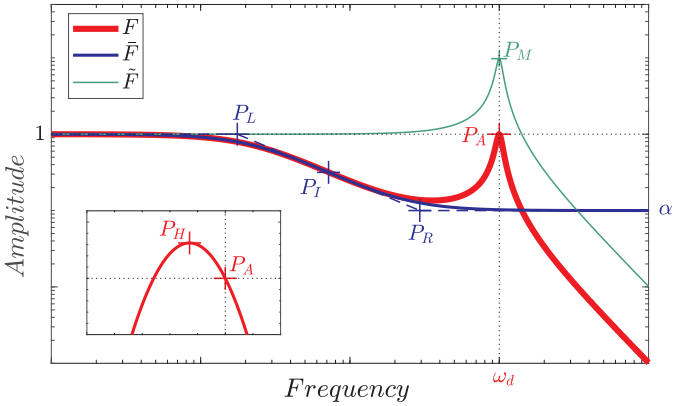

Fig. 2. Amplitude frequency response of the proposed filter (20) in logarithmic scale with the important design values and break points of its components (21) and (22).

which yields the solutions:

$$\xi_{1..4} = \pm \sqrt{\frac{1 \pm \sqrt{1 - \left| \bar{F}(j\omega_d) \right|^2}}{2}}. \tag{34}$$

Taking into account $0 < \xi < \frac{1}{\sqrt{2}}$, the only solution within the limits is given by (24), where (26) is substituted for $|\bar{F}(j\omega_d)|$. The argument shift of (20) at ω_d is given by:

$$\arg F(j\omega_d) = \operatorname{atan} \frac{-T_f(1 - \alpha)\omega_d}{\alpha T_f^2 \omega_d^2 + 1} + \operatorname{atan} \frac{-2\Omega\xi\omega_d}{\Omega^2 - \omega_d^2}. \tag{35}$$

Finally, as $\Omega > \omega_d$, (14) applies too. □

B. Robustness analysis

First, we address robustness against variation between the true and nominal target frequency ω_d. Analogously to [38], the tolerance of the control system to frequency variations of the suppressed signal is characterized by the characteristic slope of the cones observed in the magnitude-frequency curve of the sensitivity at frequency ω_d. The characteristic slope is defined as:

$$\kappa := \lim_{\Delta v \to +0} \frac{|S(j(\omega_d + \Delta v)| - |S(j\omega_d)|}{\Delta v}, \tag{36}$$

where Δv is the frequency variation. Since $S(j\omega_d) = 0$,

$$\kappa = \lim_{\Delta v \to +0} \frac{|S(j(\omega_d + \Delta v))|}{\Delta v} = |S'(j\omega_d)|. \tag{37}$$

Intuitively, the lower the κ is, the wider the cone is, implying that the sensitivity is more stagnant to the disturbance frequency and the system is less sensitive to its variations. On the contrary, higher κ values imply increased sensitivity. Consequently, in the case of rejection of periodic disturbances, one wishes to make κ as small as possible for every constituting frequency. Interestingly, an estimate of the κ value can be obtained in a simple way as follows:

Lemma 1: The value of the characteristic slope is predominantly determined by

$$\kappa \cong \tau_m + \vartheta + \frac{1}{\xi\Omega} \tag{38}$$

Proof. To simplify the notations, consider $\nu = (\tau_m + \vartheta)$. Then

$$\begin{aligned} S'(s) &= -F'(s)e^{-s\nu} + \nu F(s)e^{-s\nu} \\ &= \nu F(s)e^{-s\nu} - \left(\bar{F}'(s)\tilde{F}(s) + \bar{F}(s)\tilde{F}'(s) \right) e^{-s\nu}, \end{aligned} \tag{39}$$

where

$$\bar{F}'(s) = -\frac{T_f(1 - \alpha)}{(T_f s + 1)^2}, \tag{40}$$

$$\tilde{F}'(s) = \frac{-\Omega^2(2s + 2\xi\Omega)}{(s^2 + 2\xi\Omega s + \Omega^2)^2}. \tag{41}$$

By rearranging the polynomials in the transfer functions, Equation (39) can be rewritten as:

$$S'(s) = \nu F(s)e^{-s\nu} + F(s)e^{-s\nu} \left(\bar{H}(s) + \tilde{H}(s) \right), \tag{42}$$

where

$$\bar{H}(s) = \frac{T_f(1 - \alpha)}{(T_f s + 1)(\alpha T_f s + 1)}, \tag{43}$$

and

$$\tilde{H}(s) = \frac{2(s+\xi\Omega)}{s^2+2\xi\Omega s+\Omega^2}. \quad (44)$$

Substituting $j\omega_d$ for s in (42), due to (17), we have $F(j\omega_d)e^{-j\omega_d\nu} = 1$ and

$$S'(j\omega_d) = \nu + \bar{H}(j\omega_d) + \tilde{H}(j\omega_d). \quad (45)$$

Taking into account (25), $\tilde{H}(j\omega_d)$ can be simplified to:

$$\tilde{H}(j\omega_d) = \frac{2(\xi\Omega+j\omega_d)}{\Omega^2-\omega_d^2+2\xi\Omega j\omega_d} = \frac{2(\xi\Omega+j\omega_d)}{2\xi^2\Omega^2+2\xi\Omega j\omega_d} = \frac{1}{\xi\Omega}. \quad (46)$$

The other function reads as

$$\bar{H}(j\omega_d) = Ae^{j\Phi}, \quad (47)$$

where

$$A = \frac{T_f(1-\alpha)}{\sqrt{T_f^2\omega_d^2+1}\sqrt{\alpha^2T_f^2\omega_d^2+1}}, \quad (48)$$

and $\Phi = \operatorname{atan}(-T_f\omega_d) + \operatorname{atan}(-\alpha T_f\omega_d)$. Define $\gamma = T_f\omega_d$. Then

$$A = \frac{\gamma(1-\alpha)}{\omega_d\sqrt{\gamma^2+1}\sqrt{\alpha^2\gamma^2+1}} = \frac{1-\alpha}{\gamma\Omega\sqrt{1-2\xi^2}\sqrt{1+\frac{1}{\gamma^2}}\sqrt{\alpha^2+\frac{1}{\gamma^2}}}. \quad (49)$$

Assuming $\gamma \gg 1$, the magnitude can be approximated by

$$A \cong \frac{(1-\alpha)}{\gamma\alpha\Omega\sqrt{1-2\xi^2}}. \quad (50)$$

In order to justify neglecting the contribution of $\bar{H}(j\omega_d)$ to the magnitude of (42) as it is considered in (38), the following condition needs to be satisfied:

$$\frac{(1-\alpha)}{\gamma\alpha\Omega\sqrt{1-2\xi^2}} \ll \frac{1}{\xi\Omega}. \quad (51)$$

For $\gamma \gg 1$, the condition (23) holds and $|\bar{F}(j\omega_d)| \to \alpha$. Thus, from (24), we have

$$\xi \cong \sqrt{\frac{1-\sqrt{1-\alpha^2}}{2}}.$$

Taking this approximation into account, inequality (51) can be turned to:

$$\frac{(1-\alpha)\sqrt{\frac{1-\sqrt{1-\alpha^2}}{2}}}{\alpha\sqrt[4]{1-\alpha^2}} \ll \gamma, \quad (52)$$

which holds as the left side is upper bounded by $1/2$ for $\alpha \to 0$.

Note also that the assumption $\gamma \gg 1$ is practically meaningful. For smaller values of α, it applies directly from (23). Considering the oscillation period of the disturbance $T_d = \frac{2\pi}{\omega_d}$, the strong inequality is satisfied already for $T_f > \frac{10}{2\pi}T_d$. To achieve a filtration effect by the controller with respect to the oscillation period, the inequality should be even stronger, which justifies considering $\gamma \gg 1$.

□

Next, we address robustness against parameter variations, for which the standard H_∞ norm analysis is used. The filter has a favorable effect on the H_∞ norm of the sensitivity given in the following Lemma:

Lemma 2: Consider the filter $F(s)$ given by (20)–(25). Then the H_∞ norms of the sensitivity functions (11) and (12) satisfy

$$||S(j\omega)|| < 2+\epsilon, \quad (53)$$

$$||T(j\omega)|| < 1+\epsilon, \quad (54)$$

where $\epsilon \ll 1$.

Proof. For the complementary sensitivity (12), it is easy to observe that $||T(j\omega)|| = ||F(j\omega)||$. Define

$$\delta(\omega) = |\bar{F}(j\omega)| - \alpha. \quad (55)$$

Then, the filter magnitude can be expressed as

$$|F(j\omega)| = |\tilde{F}(j\omega)|(\alpha+\delta(\omega)). \quad (56)$$

If for a fixed α, the parameter T_f is selected to satisfy the condition (23), then the breaking point P_R of (26) is located to the left of ω_d. As a consequence, in the vicinity of ω_d, one has:

$$|\tilde{F}(j\omega)|\alpha \gg |\tilde{F}(j\omega)|\delta(\omega). \quad (57)$$

Thus, for the peak value point $P_H = [\omega_H, 1+\epsilon]$ of $|F(j\omega)|$, visualized in sub-figure of Fig. 2 it follows that $\epsilon \ll 1$ and the condition (54) holds.

Consequently, as $||S(j\omega)|| = ||1-T(j\omega)||$ with a potential maximum at $2+\epsilon$, the condition (53) follows. □

The above given bounds on H_∞ already guarantee a certain robustness level. In the case study below, it will be shown that, by an appropriate choice of T_f and α, the robustness measures can even be decreased.

C. Extended filter design

Although the main results are derived for suppressing a single harmonic disturbance, the method can be extended to suppress multiple frequency harmonic disturbance similar to that of [39]. Here, we propose a filter for the IMC scheme to compensate the effect of a harmonic disturbance (2) with two frequencies.

Assume two filter-delay pairs $[F_d(s), \vartheta_d]$ and $[F_s(s), \vartheta_s]$ tuned independently according to Propositions 1 and 2 to target frequencies ω_d and ω_s, respectively. With this assumption, one merges the filters to

$$F_D(s) = F_d(s)e^{-s\vartheta_d} + F_s(s)e^{-s\vartheta_s} - F_d(s)F_s(s)e^{-s(\vartheta_d+\vartheta_s+\tau_m)}. \quad (58)$$

Proposition 3: With the assumptions above, the IMC controller (with the scheme in Fig. 1) in the form

$$C(s) = \frac{1}{G_m(s)}F_D(s) \quad (59)$$

fully compensates the double harmonic disturbance (2).

Proof. By applying the controller (59), the nominal sensitivity function of the IMC scheme reads as:

$$S(s) = 1 - F_d(s)e^{-s(\vartheta_d+\tau_m)} - F_s(s)e^{-s(\vartheta_s+\tau_m)} + F_d(s)F_s(s)e^{-s(\vartheta_d+\vartheta_s+2\tau_m)} = S_d(s)S_s(s), \quad (60)$$

where $S_d(j\omega)$ and $S_s(j\omega)$ are the sensitivities (11) substituted with $[F_d(s), \vartheta_d]$ and $[F_s(s), \vartheta_s]$, respectively. Consequently, it is easy to see that the conditions $S(j\omega_d) = 0$ and $S(j\omega_s) = 0$ are satisfied simultaneously, which implies a complete compensation of the double harmonic disturbance. □

The aforementioned method can be readily generalized to increase the number of covered frequencies. However, it must be noted that each added filter-delay pair contributes to the overall delay of the resulting filter. An alternative approach to target multiple frequencies has recently been proposed in [40]. Compared to the fully analytic design method presented here, the one of [40] is based on loop shaping with spectral constraints. Besides, a multi-parameter distributed delay is involved in the controller, which increases its structural complexity compared to (7).

It can be easily seen from (60) that the H_∞ norm of the sensitivity with combined filters satisfies

$$||S(j\omega)|| \leq ||S_d(j\omega)|| \, ||S_s(j\omega)|| \, . \quad (61)$$

Similarly, by taking the derivative of (60) and substituting it into (37) with frequency ω_i, we can find the characteristic slopes by

$$\kappa_i = |S_i'(j\omega_i)| \, |S_k(j\omega_i)| \, , \quad (62)$$

where $i, k \in [d, s]$, $i \neq k$.

Secondly, an extended filter is proposed for a single frequency harmonic disturbance with an enhanced robustness against mismatch between nominal and true excitation frequency.

Proposition 4: Assume the filter-delay pair $[F(s), \vartheta]$ is tuned to satisfy the conditions (13)-(16) and (20)–(25) to target the frequency ω_d. Then the controller

$$C(s) = \frac{1}{G_m(s)} F_R(s), \quad (63)$$

with the filter

$$F_R(s) = 2F(s)e^{-s\vartheta} - F(s)F(s)e^{-s(2\vartheta+\tau_m)} \quad (64)$$

applied at the IMC scheme in Fig. 1 results in an enhanced robustness against frequency ω_d variation with characteristic slope $\kappa = 0$.

Proof. Applying the filter (64) the nominal sensitivity function of the IMC scheme reads as

$$S(s) = 1 - 2F(s)e^{-s(\vartheta+\tau_m)} + F(s)F(s)e^{-s(2\vartheta+2\tau_m)}, \quad (65)$$

which can be turned to

$$S(s) = \left(1 - F(s)e^{-s(\vartheta+\tau_m)}\right)^2. \quad (66)$$

Thus, when the filter-delay pair $[F(s), \vartheta]$ is designed to satisfy the conditions (13)-(16) and (20)–(25) to target the frequency ω_d,

then

$$S(j\omega_d) = 0, \quad (67)$$

$$S'(j\omega_d) = 0 \quad (68)$$

are both satisfied. Due to (37), we have $\kappa = 0$ implying enhanced robustness against variation of ω_d. □

IV. Experimental case study

In order to validate the proposed methods experimentally, we designed and built a mechatronic set-up with the aim to mimic dominant technological aspects of the eccentricity compensation of hot rolling process, which motivated the presented research. In particular, an inner control loop is included to provide a higher order well-damped dynamics, similarly as it is in the hydraulic inner control subsystem of the rolling gap. Besides, we assume a long delay at the system input consisting of a delay approximating the dead-time τ_d of the inner control loop and dominant delay τ which is known exactly.

The scheme of the proposed set-up and inner control loops is shown in Fig. 3. It consists of a series of two mechanical oscillators, described by the model

$$m_1\ddot{x}_1(t) + (c_1 + c_2)\dot{x}_1(t) + (k_1 + k_2)x_1(t) = c_2\dot{x}_2(t) + k_2x_2(t) + u_1(t) - u_2(t), \quad (69)$$

$$m_2\ddot{x}_2(t) + c_2\dot{x}_2(t) + k_2x_2(t) = c_2\dot{x}_1(t) + k_2x_1(t) + u_2(t), \quad (70)$$

where x_1, x_2 denote the positions of the bodies, and u_1, u_2 control forces. The parameters m_1, m_2 denote masses of the bodies, k_1, k_2 stiffness and c_1, c_2 damping of the links. The system output to be controlled by the IMC scheme is the position of the main body x_1, i.e.

$$y(t) = x_1(t). \quad (71)$$

In order to turn the oscillatory fourth-order system into a well-damped system which can be approximated by (1), the inner control loops are applied as

$$u_1(t) = r_{o1}(u(t) - x_1(t)) - r_{d1}\dot{x}_1(t), \quad (72)$$

$$u_2(t) = r_{o2}(d_{\text{set}}(t) - \Delta x(t)) - r_{d2}\Delta\dot{x}(t), \quad (73)$$

where $\Delta x(t) = x_2(t) - x_1(t)$, u is the control input of the IMC scheme, and d_{set} is the set-point of the disturbance - the position Δx generating the disturbance force effect to the body with m_1. The parameters to be tuned are the proportional r_{o1}, r_{o2} and derivative r_{d1}, r_{d2} gains.

A. Instrumentation and mechatronic design

The implementation of the experimental set-up depicted in Fig. 3 is shown in Fig. 4, together with the implementation of the control scheme. The two carts with m_1 and m_2 are interconnected with a pair of springs. Another pair of springs is used to fix the main body cart (m_1) to the left and right base elements. Both the carts slide on rails - the m_2-cart rails are fixed to the m_1-cart while the rails of m_1-cart are fixed

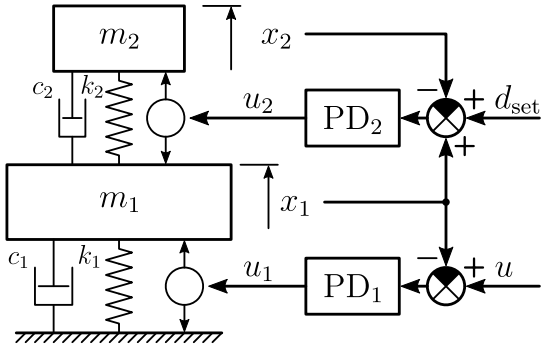

Fig. 3. Scheme of the experimental set-up and inner control loops

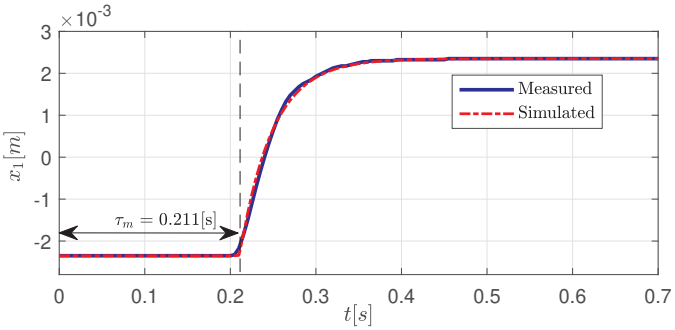

Fig. 5. Transient response of the inner control loop of the set-up and its approximation by the model (1), with the visualization of the identified input delay $\tau_m = 0.211[s]$

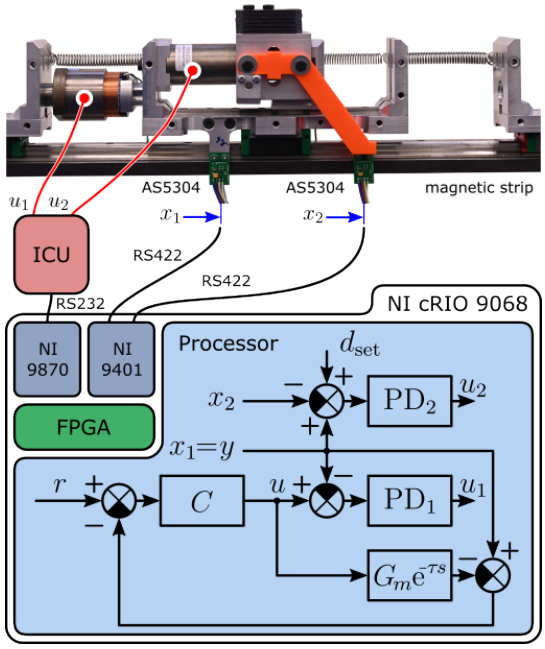

Fig. 4. Mechatronic implementation of the set-up and its control system

to the base. The carts are actuated by two voice-coil linear motors generating forces u_1 and u_2. The damping in the cart dynamics is mainly caused by the viscous friction between the bearings and the rails. The positions x_1, x_2 of the carts are measured by incremental position sensors.

The discrete version of the proposed IMC control scheme for harmonic disturbance compensation depicted in Fig. 1, obtained by zero-order hold method, was implemented in LabVIEW™ and performed using the CompactRIO controller with 1 kHz sampling. The CompactRIO controller consists of a microprocessor and an FPGA module. The microprocessor computes the nominal forces u_1 and u_2. The control action u_1 is exerted by the main control loop composed of the master IMC scheme and inner PD loop. The other control action u_2 generating the disturbance is exerted by the other PD control loop. The FPGA module is used to (i) read the quadrature incremental signals RS-422 from position sensors via digital input-output card NI9401, (ii) decoding to increment or decrement the relative positions x_1 and x_2, and (iii) command an industrial control unit (ICU) to control voice-coil motors. Both voice-coil motors run in the force regime. The nominal value of the forces u_1 and u_2 to be applied on the movable carts is transmitted from serial card NI9870 via RS-232 into the industrial control unit. Both the reading of the quadrature signals together with its decoding and the transmission of the reference forces via RS-232 were also implemented in LabVIEW™.

B. Parameter Identification

In the model (69)-(70) the masses $m_1 = 1.1\,\text{kg}$, $m_2 = 0.514\,\text{kg}$ were obtained by weighting the carts. The stiffness coefficients $k_1 = 1768\,\text{N m}^{-1}$, $k_2 = 424\,\text{N m}^{-1}$, were measured utilizing the force gauge, while the damping coefficients $c_1 = 4.43\,\text{N s m}^{-1}$, $c_2 = 2.41\,\text{N s m}^{-1}$ were determined experimentally from a series of responses. The parameters of the PD controllers have been pre-tuned analytically by using the standard pole placement methodology and, subsequently, adjusted experimentally to obtain the well-damped response shown in Fig. 5. Consequently, the approximate model (1) parameters have been assessed as $K = 0.47$, $T = 0.038\,\text{s}$ and $\tau_d = 0.011\,\text{s}$. As the identified delay is relatively small, it was software-wise increased by delaying the variable $u(t-\tau)$ with $\tau = 0.2\,\text{s}$. As it can be seen in Fig. 5, the model fits the measured response fairly well. Furthermore, it is easy to observe that the overall delay of the system $\tau_m = 0.211\,\text{s}$ is substantial with respect to the time constant T. Consequently, its robust compensation by the IMC scheme is crucial to achieve favourable responses.

C. Single-frequency harmonic disturbance compensation

The performance of the proposed IMC control scheme is initially validated for the single harmonic disturbance (3) with $\omega_d = 8\,\text{Hz}$ ($50.27\,\text{s}^{-1}$). The first step in designing the filter (20) according to Proposition 2 is selecting α and T_f. Based on the theoretical analysis provided above, we select $\alpha = 0.3$ and $T_f = 1\,\text{s}$, providing $\gamma = T_f\omega_d = 50.27$ safely satisfying the required inequality $\gamma \gg 1$. By (24) and (25), the other two parameters result as $\xi = 0.152$ and $\Omega = 51.47\,\text{s}^{-1}$. The last parameter of the controller (7) is the delay $\vartheta = 0.010\,\text{s}$ determined from (15).

Suitability of the selected α, T_f setting is confirmed in Fig. 6, where the considered H_∞ and κ robustness measures

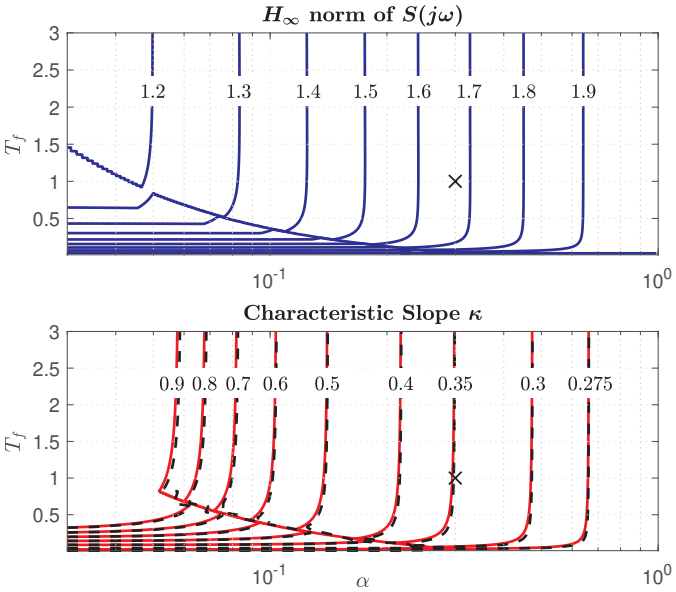

Fig. 6. Robustness analysis of the sensitivity function (11) with the filter $F(s)$ proposed for the set-up and single harmonic disturbance with $\omega_d = 8\,\mathrm{Hz}$ by Propositions 1 and 2. (**Top**) H_∞ of (11). (**Bottom**) Characteristic slope κ given by (37) (solid) and its approximation (38) (dashed)

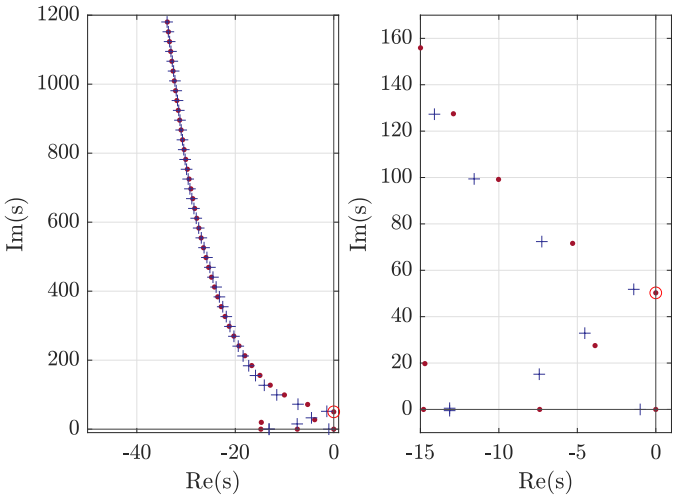

Fig. 7. Pole (+) - Zero (•) spectrum of the non-ideal sensitivity (9); ∘ - desired position of the dominant zero at $j\omega_d$. (**Left**) Overall distribution (**Right**) Close-up view on the zeros compensating the harmonics.

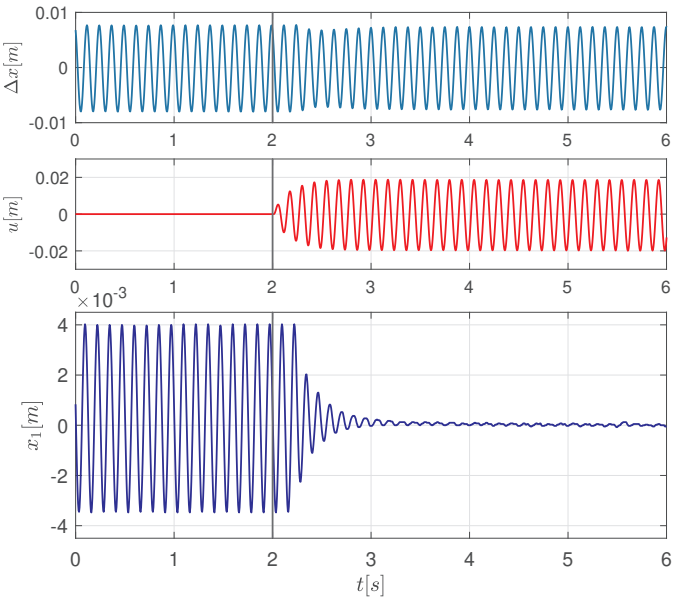

Fig. 8. Experimental results for single harmonic ($\omega_d = 8\,\mathrm{Hz}$) disturbance compensation. The IMC loop with filter (20) activated at $t = 2s$.

are shown with respect to α and T_f (The parameter couple $[\alpha, T_f]$ selected for the experiments is denoted by $\times$ marker in Fig. 6). The measures were obtained numerically from $S(j\omega)$ by varying controller settings. Numerical determination of H_∞ was done by sweeping the frequency over a dense and sufficiently wide range. In the κ sub-figure, also the approximation (38) is shown. An almost perfect match is confirmed with exact κ determined from (37). The figure clearly shows that, from some value of T_f, smaller values of α result in a smaller H_∞ norm and a larger κ, and vice versa. Notice also that from a certain value of T_f, the measures remain almost constant. It indicates that a further increase of T_f is dispensable.

Prior to the experimentation, the stability of the control system with inevitable plant-model mismatch is assessed by checking the spectrum of the non-ideal sensitivity (9) substituted with the identified first-order model $G_m(s)$, overall delay $\tau_m = 0.211\,\mathrm{s}$, tuned low-pass filter and the exact system model

$$G_i(s) = \frac{y(s)}{u(s)} = \frac{513.6s^2 + 4.091\,10^4 s + 5.093\,10^5}{s^4 + 165s^3 + 6384s^2 + 1.348\,10^5 s + 1.084\,10^6}, \quad (74)$$

analytically obtained from (69)-(73) together with the added delay $\tau = 0.2\,\mathrm{s}$. Thus, the delays τ_m and τ are not identical and $G_i(s)$ does not share the same structure as its model $G_m(s)$. In Fig. 7, the spectra of poles and zeros for the non-ideal sensitivity (9), computed by QPmR algorithm [41], are shown. As can be seen, the dominant zero is placed, as required, at $j\omega_d$. The rest of the zeros is located to the left, forming the retarded chain [42]. Regarding the system's rightmost poles, they are all located safely to the left of the imaginary axis, which implies the closed loop stability. As it can also be seen, the poles also form a retarder chain which tends to match the chain of zeros at high frequencies.

The experimental results are shown in Figs. 8 and 9. Fig. 8 demonstrates almost ideal harmonic disturbance compensation. As it can be seen, after activating the IMC loop at $t = 2\,\mathrm{s}$, it generates the control action u which, after propagating through the overall delay $\tau_m = 0.211\,\mathrm{s}$ and remaining loop dynamics, silences the main cart $y = x_1$ position to the level of measurement noise. Meanwhile, the other cart with position x_2 monotonously oscillates, causing periodic force disturbance at the main cart. In Fig. 9, a response to a reference r step is shown under the periodic disturbance compensation. It demonstrates a very good reference tracking feature towards zero residual control error[1]. Let us note that the almost ideal

[1]Video record of the experiments is shown at https://control.fs.cvut.cz/en/aclab/experiments/harmcomp

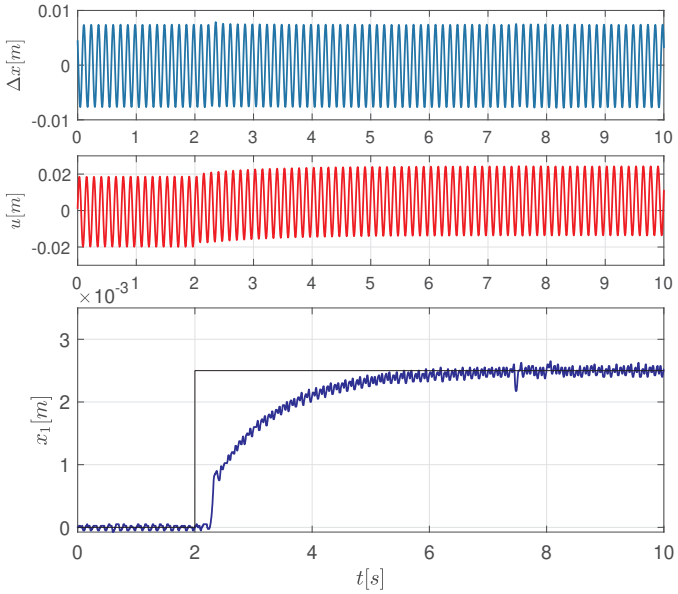

Fig. 9. Experimental results for set-point response under single harmonic ($\omega_d = 8\,\mathrm{Hz}$) disturbance compensation, IMC loop with filter (20).

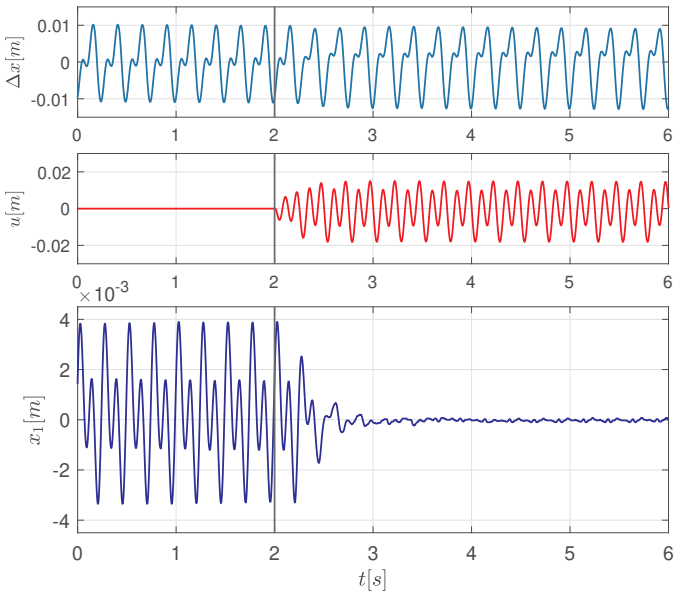

Fig. 10. Experimental results for double harmonic ($\omega_d = 8\,\mathrm{Hz}$, $\omega_s = 4\,\mathrm{Hz}$) disturbance compensation. The IMC loop with filter (58) turned on at $t = 2\,\mathrm{s}$.

experimental results, achieved under approximating the fourth-order dynamics by first-order dynamics and under the presence of unmodelled nonlinearities, such as dry friction, demonstrate enhanced robustness of the scheme imposed by the properly configured filter.

D. Double-frequency harmonic disturbance compensation

Secondly, the IMC control scheme with the controller (59) and extended filter-delay structure (58) is used to target double-frequency signal (2) with $\omega_d = 8\,\mathrm{Hz}$ ($50.27\,\mathrm{s}^{-1}$) and $\omega_s = 4\,\mathrm{Hz}$ ($25.13\,\mathrm{s}^{-1}$). For both the filters, the parameters $\alpha = 0.3$ and $T_f = 1\,\mathrm{s}$ are considered. Thus, the filter-delay pair $[F_1(s), \vartheta_1]$ is the same as for the above single frequency case. For the filter $F_2(s)$, we have $\xi = 0.153$ and $\Omega = 25.74\,\mathrm{rad/s}$ by (24) and (25). By (15), we have $\vartheta_2 = 0.229s$. The experimental results shown in Fig. 10 and Fig. 11 reveal remarkably good performance towards double-harmonic disturbance compensation by the IMC scheme with the extended filter. Compared to the single frequency compensation, a slight overshoot can be observed in Fig. 11. It results from the overall filter composition (58) and cannot be removed unless the filter form is modified. It could possibly be lowered by considering longer T_f values. This would, however, lead to slower control actions not only for the reference but also for the disturbance, which is undesirable. Alternatively, the overshoot can be removed by including a reference pre-filter, which is commonly used in industrial control schemes.

E. Robust single-frequency harmonic disturbance compensation

Finally, we apply the IMC scheme with controller (63) and robust filter structure (64) considering $F(s)$ and ϑ taken from the Sub-section IV-C to target $\omega_d = 8\,\mathrm{Hz}$. The results in Figs. 12 and 13 show very good disturbance compensation in the nominal case as well as good reference tracking with a

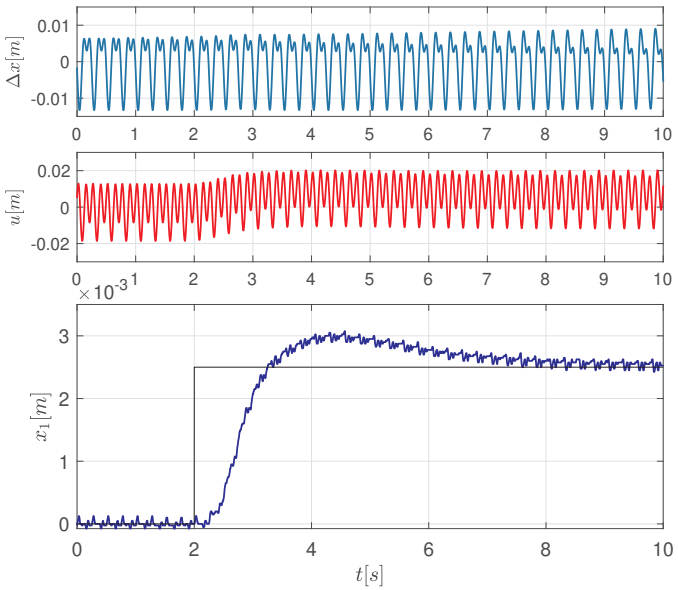

Fig. 11. Experimental results for set-point response under double harmonic ($\omega_d = 8\,\mathrm{Hz}$, $\omega_s = 4\,\mathrm{Hz}$) disturbance compensation, IMC loop with filter (58).

slight overshoot, which can be adjusted analogously to the double-frequency disturbance scheme discussed above. The enhanced robustness against ω_d variation is shown at the bottom of Fig. 14. Experimentally, the residual amplitude was determined for IMC with nominal filter structure (20) and the robust filter structure (64) for the frequency range $\omega \in [7.2, 8.8]$ Hz. In Fig. 14, next to the measured characteristics, the characteristics obtained from the transfer functions are shown. From the comparison, a very good match can be seen. The figure also confirms the enhanced robustness against ω_d mismatch. The characteristic slope of the first configuration is obtained as $\kappa = 0.349$ and agrees with both estimated and measured response. For the double frequency case, the characteristic slopes for frequencies 4Hz and 8 Hz are found to

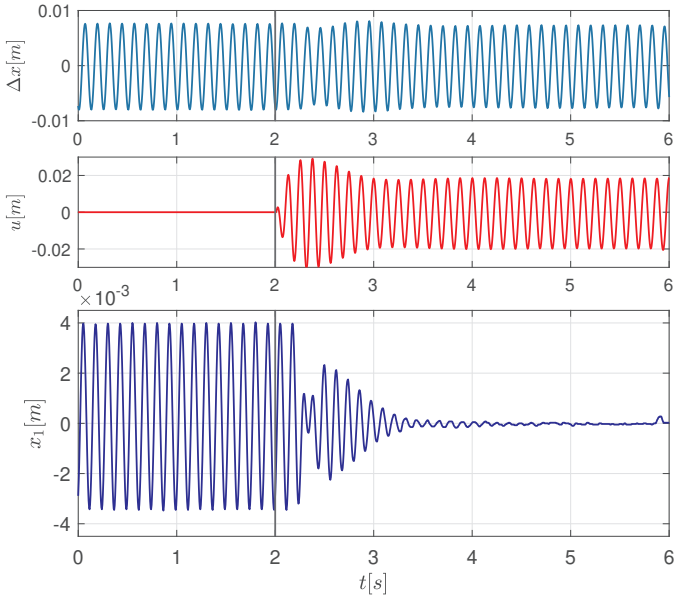

Fig. 12. Experimental results for single harmonic ($\omega_d = 8\,\text{Hz}$) disturbance compensation. The IMC loop with robust filter (64) turned on at $t = 2s$.

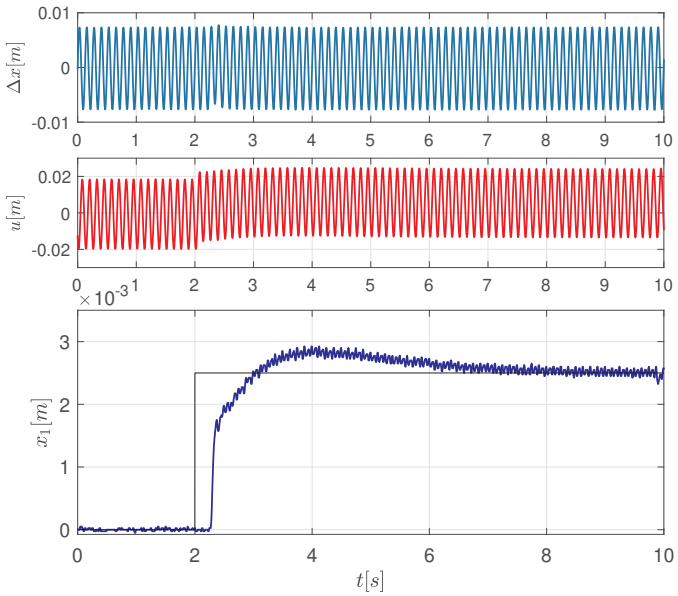

Fig. 13. Experimental results for set-point response under single harmonic ($\omega_d = 8\,\text{Hz}$, IMC loop with robust filter (64).

be $\kappa = 0.473$ and $\kappa = 0.312$, respectively. For the robust filter configuration, $\kappa = 0$ can be observed as predicted. Finally, the sensitivity magnitudes for the considered cases are shown in the upper part of Fig. 14. Next to the stop-band feature at the targeted frequencies, the maxima of the magnitudes are of interest. It reveals a smaller robustness against parameter variation for the sensitivity function with the extended filter (64).

V. Conclusions

A complete analytical and practical method to compensate harmonic disturbance of a system with long dead-time was proposed, analysed with respect to robustness measures and experimentally validated. The method is based on an extended

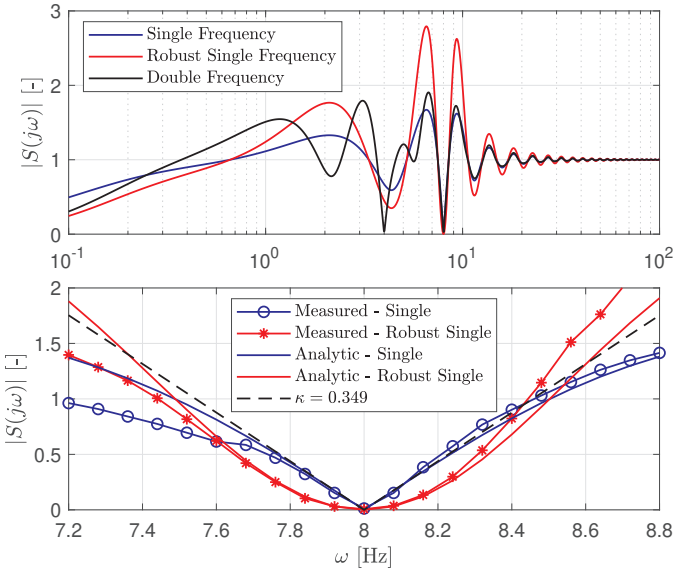

Fig. 14. Amplitude responses of the sensitivity function $S(j\omega)$ with the considered harmonic disturbance cases (**Top**) Simulated on a large frequency range. (**Bottom**) Comparison of measured and simulated in the vicinity of the target mode $\omega_d = 8\,\text{Hz}$.

internal model control scheme. A crucial task stems in the filter design with two optional parameters allowing to balance robustness against variation of the frequency of oscillation and the robustness against parameter variation based on H_∞ norm of sensitivity function.

The main results have been derived for a single harmonic disturbance compensation. Following that, the scheme is extended to double frequency harmonic disturbance compensation. By the later extended scheme, enhanced robustness against single frequency cases can be achieved. The presented research was motivated by the eccentricity compensation of the hot-rolling process, where the dead-time plays an important role in the dynamics. The compensation of such dead-time is necessary in order to have a sufficiently fast controller to perform the harmonic compensation efficiently. Note that the standard repetitive control scheme does not involve the delay compensation. Thus, the infinite dimensionality of the loop dynamics needs to be taken into account in the repetitive controller design, which is not the case with the proposed IMC method.

In order to validate the theoretical results experimentally, a mechatronic set-up has been proposed and implemented. The proposed control system consisting of the extended IMC scheme and inner PD control loops has been implemented in LabVIEW™ on the industrial NI-CompactRIO platform. The experimental results revealed outstanding ability in simultaneous compensation of both long dead-time and harmonic disturbance. Validation on the hot-rolling process is the next challenging task.

Appendix

In order to determine the inflection point (28) and braking points (29) of the amplitude response of the filter (21) in the

logarithmic scale, as shown in Fig. 2, we express the filter magnitude as

$$\log|\bar{F}(j\omega)| = \frac{1}{2}\left(\log(\alpha^2 T_f^2\omega^2+1) - \log(T_f^2\omega^2+1)\right). \tag{75}$$

Substituting $\varpi = \log\omega$ leads to

$$A(\varpi) = \frac{1}{2}\left(\log(\alpha^2 T_f^2 10^{2\varpi}+1) - \log(T_f^2 10^{2\varpi}+1)\right). \tag{76}$$

The inflection point (28), is determined by solving $\frac{d^2A(\varpi)}{d\varpi^2} = 0$, which can be simplified to the condition

$$10^{4\varpi}T_f^4\alpha^2 - 1 = 0. \tag{77}$$

The solution of (77) given by $\varpi_I = \log\frac{1}{T_f\sqrt{\alpha}}$ implies the inflection point coordinates $\omega_I = \frac{1}{T_f\sqrt{\alpha}}$ and $|\bar{F}(j\omega_I)| = \sqrt{\alpha}$.

Evaluating $\frac{dA(\varpi)}{d\varpi}|_{\varpi=\varpi_I} = \frac{\alpha-1}{\alpha+1}$ leads to the tangent at the inflection point

$$\log\Phi(\omega) = \log\sqrt{\alpha} + \frac{\alpha-1}{\alpha+1}\left(\log\omega - \log\frac{1}{T_f\sqrt{\alpha}}\right), \tag{78}$$

which can be simplified to

$$\log\Phi(\omega) = \log\sqrt{\alpha} + \frac{\alpha-1}{\alpha+1}\log(T_f\sqrt{\alpha}\omega). \tag{79}$$

Thus, the points (29) can be obtained as solution of (79) by substituting $\Phi(\omega) = 1$ for P_L and $\Phi(\omega) = \alpha$ for P_R, respectively.

REFERENCES

[1] B. A. Francis and W. M. Wonham, "The internal model principle of control theory," *Automatica*, vol. 12, no. 5, pp. 457–465, 1976.

[2] T. Inoue, M. Nakano, T. Kubo, S. Matsumoto, and H. Baba, "High accuracy control of a proton synchrotron magnet power supply," *IFAC Proceedings Volumes*, vol. 14, no. 2, pp. 3137–3142, 1981.

[3] S. Hara, Y. Yamamoto, T. Omata, and M. Nakano, "Repetitive control system: A new type servo system for periodic exogenous signals," *IEEE Transactions on automatic control*, vol. 33, no. 7, pp. 659–668, 1988.

[4] M. Tomizuka, T.-C. Tsao, and K.-K. Chew, "Analysis and synthesis of discrete-time repetitive controllers," *Journal of Dynamic Systems, Measurement, and Control*, vol. 111, no. 3, pp. 353–358, 1989.

[5] T. Inoue, "Practical repetitive control system design," in *29th IEEE Conference on Decision and Control*, 1990, pp. 1673–1678.

[6] M. Steinbuch, S. Weiland, and T. Singh, "Design of noise and period-time robust high-order repetitive control, with application to optical storage," *Automatica*, vol. 43, no. 12, pp. 2086–2095, 2007.

[7] G. Pipeleers, B. Demeulenaere, J. De Schutter, and J. Swevers, "Robust high-order repetitive control: optimal performance trade-offs," *Automatica*, vol. 44, no. 10, pp. 2628–2634, 2008.

[8] X.-D. Li, T. W. Chow, and J. K. Ho, "Quasi-sliding mode based repetitive control for nonlinear continuous-time systems with rejection of periodic disturbances," *Automatica*, vol. 45, no. 1, pp. 103–108, 2009.

[9] Y. Lin, C. Chung, and T. Hung, "On robust stability of nonlinear repetitive control system: Factorization approach," in *1991 IEEE American Control Conference*, 1991, pp. 2646–2647.

[10] T. Omata, S. Hara, and M. Nakano, "Nonlinear repetitive control with application to trajectory control of manipulators," *Journal of Robotic systems*, vol. 4, no. 5, pp. 631–652, 1987.

[11] K. Omura, H. Ujikawa, O. Kaneko, Y. Okano, S. Yamamoto, H. Imanari, and T. Horikawa, "Attenuation of roll eccentric disturbance by modified repetitive controllers for steel strip process with transport time delay," *IFAC-PapersOnLine*, vol. 48, no. 17, pp. 131–136, 2015.

[12] B. A. Güvenç and L. Güvenç, "Robust repetitive controller design in parameter space," *Journal of Dynamic Systems, Measurement and Control*, vol. 182, no. 2, pp. 406–413, 2006.

[13] K. Srinivasan and F.-R. Shaw, "Analysis and Design of Repetitive Control Systems Using the Regeneration Spectrum," *Journal of Dynamic Systems, Measurement, and Control*, vol. 113, no. 2, pp. 216–222, 06 1991. [Online]. Available: https://doi.org/10.1115/1.2896368

[14] K. Watanabe and K. Yamada, "Repetitive control of time-delay systems," in *29th IEEE Conference on Decision and Control*, 1990, pp. 1685–1690.

[15] Z. Zhang, B. Chu, Y. Liu, Z. Li, and D. H. Owens, "Multimuscle functional-electrical-stimulation-based wrist tremor suppression using repetitive control," *IEEE/ASME Transactions on Mechatronics*, 2022.

[16] W.-W. Huang, C. Hu, and L.-M. Zhu, "Robust repetitive control of nanopositioning stages using the spectrum-selection filter with narrow passbands," *IEEE/ASME Transactions on Mechatronics*, 2022.

[17] L. Li, Z. Chen, S. S. Aphale, and L. Zhu, "Fractional repetitive control of nanopositioning stages for high-speed scanning using low-pass fir variable fractional delay filter," *IEEE/ASME Transactions on Mechatronics*, vol. 25, no. 2, pp. 547–557, 2020.

[18] Y. Tao, Z. Zhu, Q. Xu, H.-X. Li, and L. Zhu, "Tracking control of nanopositioning stages using parallel resonant controllers for high-speed nonraster sequential scanning," *IEEE Transactions on Automation Science and Engineering*, vol. 18, no. 3, pp. 1218–1228, 2020.

[19] H. Tian, P. Y. Li, and J. D. Van de Ven, "Valve timing control for a digital displacement hydraulic motor using an angle-domain repetitive controller," *IEEE/ASME Transactions on Mechatronics*, vol. 24, no. 3, pp. 1306–1315, 2019.

[20] E. L. O. Batista, M. R. Barghouthi, and E. M. de Oliveira Lopes, "A novel adaptive scheme to improve the performance of feedforward active vibration control systems," *IEEE/ASME Transactions on Mechatronics*, 2021.

[21] J. Ghosh and B. Paden, "Nonlinear repetitive control," *IEEE Transactions on Automatic Control*, vol. 45, no. 5, pp. 949–954, 2000.

[22] G. Fedele and A. Ferrise, "Periodic disturbance rejection with unknown frequency and unknown plant structure," *Journal of the Franklin Institute*, vol. 351, no. 2, pp. 1074–1092, 2014.

[23] C. Kinney and R. De Callafon, "An adaptive internal model-based controller for periodic disturbance rejection," *IFAC Proceedings Volumes*, vol. 39, no. 1, pp. 273–278, 2006.

[24] H.-Q. Zhou, Q.-G. Wang, and L. Min, "Modified smith predictor design for periodic disturbance rejection," *ISA transactions*, vol. 46, no. 4, pp. 493–503, 2007.

[25] G. Pipeleers, B. Demeulenaere, and J. Swevers, *Optimal linear controller design for periodic inputs*. Springer, 2009, vol. 394.

[26] W. Kim, D. Shin, D. Won, and C. C. Chung, "Disturbance-observer-based position tracking controller in the presence of biased sinusoidal disturbance for electrohydraulic actuators," *IEEE Transactions on Control Systems Technology*, vol. 21, no. 6, pp. 2290–2298, 2013.

[27] A. Bazaei, Y. K. Yong, and S. R. Moheimani, "Combining spiral scanning and internal model control for sequential afm imaging at video rate," *IEEE/ASME Transactions on Mechatronics*, vol. 22, no. 1, pp. 371–380, 2016.

[28] C. K. Yuksel, J. Bušek, S.-I. Niculescu, and T. Vyhlídal, "Internal model controller to attenuate periodic disturbance of a first-order time-delay system," in *2021 IEEE European Control Conference (ECC)*, 2021, pp. 81–86.

[29] B. Betlem and B. Roffel, *Process dynamics and control: modeling for control and prediction*. John Wiley & Sons, 2007.

[30] D. E. Seborg, T. F. Edgar, D. A. Mellichamp, and F. J. Doyle III, *Process dynamics and control*. John Wiley & Sons, 2016.

[31] R. C. Panda, *Introduction to PID controllers: theory, tuning and application to frontier areas*. BoD–Books on Demand, 2012.

[32] Z. Song, C. Liu, H. Zhao, and R. Huang, "Nonlinear force and vibration analysis of an interior permanent magnet synchronous generator with eccentricity detection," *IEEE/ASME Transactions on Mechatronics*, 2021.

[33] F. Evestedt, J. J. Perez-Loya, C. J. D. Abrahamsson, and U. Lundin, "Mitigation of unbalanced magnetic pull in synchronous machines with rotating exciters," *IEEE Transactions on Energy Conversion*, vol. 36, no. 2, pp. 812–819, 2020.

[34] T. Vyhlídal and P. Zítek, "Control system design based on a universal first order model with time delays," *Acta Polytechnica*, vol. 41, no. 4-5, 2001.

[35] C. E. Garcia and M. Morari, "Internal model control. a unifying review and some new results," *Industrial & Engineering Chemistry Process Design and Development*, vol. 21, no. 2, pp. 308–323, 1982.

[36] Y.-S. Lu, "Internal model control of lightly damped systems subject to periodic exogenous signals," *IEEE Transactions on Control Systems Technology*, vol. 18, no. 3, pp. 699–704, 2009.

[37] Q.-G. Wang, T. H. Lee, and L. Chong, *Relay feedback: analysis, identification and control*. Springer Science & Business Media, 2002.
[38] T. Vyhlídal, D. Pilbauer, B. Alikoç, and W. Michiels, "Analysis and design aspects of delayed resonator absorber with position, velocity or acceleration feedback," *Journal of Sound and Vibration*, vol. 459, p. 114831, 2019.
[39] S. S. Garimella and K. Srinivasan, "Application of Repetitive Control to Eccentricity Compensation in Rolling," *Journal of Dynamic Systems, Measurement, and Control*, vol. 118, no. 4, pp. 657–664, 12 1996.
[40] C. K. Yuksel, J. Bušek, T. Vyhlídal, S.-I. Niculescu, and M. Hromčík, "Internal model control with distributed-delay-compensator to attenuate multi-harmonic periodic disturbance of time-delay system," in *2021 60th IEEE Conference on Decision and Control (CDC)*, 2021, pp. 5477–5483.
[41] T. Vyhlidal and P. Zítek, "Mapping based algorithm for large-scale computation of quasi-polynomial zeros," *IEEE Transactions on Automatic Control*, vol. 54, no. 1, pp. 171–177, 2009.
[42] G. Stépán, *Retarded dynamical systems: stability and characteristic functions*. Longman Scientific & Technical, 1989.

Can Kutlu Yüksel received the M.Sc. (2019) in Instrumentation and Control Engineering from the Faculty of Mechanical Engineering, Czech Technical University in Prague, Czech Republic. He is currently pursuing his Ph.D under FME - CTU and Laboratoire des Signaux et Systèmes (L2S), CentraleSupelec, University of Paris-Saclay, Paris, France. His research interests include frequency-based methods for time-delay systems, periodic regulation problems and applied control theory.

Tomáš Vyhlídal graduated in Automatic Control and Engineering Informatics in 1998 and received Ph.D. in Control and Systems Engineering in 2003, both from the Faculty of Mechanical Engineering (FME), Czech Technical University in Prague (CTU). In 2012, he became professor at CTU in the subject of Control and Systems Engineering. Since 2000, he has been with the Dept. of Instrumentation and Control Eng. (dept. head since 2019), FME – CTU, and since 2015 also with the Czech Institute of Informatics, Robotics and Cybernetics, CIIRC - CTU. His research interests include spectral analysis and control design of time-delay systems, algebraic control design, mathematical modelling and applied control theory. He has been a member of the IFAC Technical Committee for Linear Control Systems since 2013, vice-chair for industry since 2017.

Jaroslav Bušek received the B.Sc. degree in Information and automation technology (2009), M.Sc. degree in Instrumentation and control engineering (2011) and Ph.D. in Technical cybernetics (2019), all degrees from the Faculty of Mechanical Engineering (FME), Czech Technical University (CTU), Prague, Czech Republic. His work is focused at anti-windup strategies for time-delay control systems and flexible systems control. He is also a member of research team focusing on application of advanced computational methods, design procedures and innovative algorithms in development, production and control of mechanical and mechatronic systems at Czech Institute of Informatics, Robotics and Cybernetics (CIIRC).

Milan Anderle was born in České Budějovice, Czech Republic, in 1984. He graduated in cybernetics and measurements in 2008 and received the Ph.D. degree in control engineering and robotics in 2016, both from the Faculty of Electrical Engineering, Czech Technical University, Prague. His Ph.D. thesis on topic Nonlinear control of underactuated walking robot was awarded by Dean's Award for the Dissertation thesis. His research interests cover applications of input shapers for control of multi-body systems and nonlinear control laws design for underactuated biped walking robots.

Silviu-Iulian Niculescu received the B.S. degree from the Polytechnical Institute of Bucharest, Romania, the M.Sc., and Ph.D. degrees from the Institut National Polytechnique de Grenoble, France, and the French Habilitation (HDR) from Université de Technologie de Compiègne, all in Automatic Control, in 1992, 1993, 1996, and 2003, respectively. He is currently Research Director at CNRS (French National Center for Scientific Research), L2S (Laboratory of Signals and Systems), a joint research unit of CNRS with CentraleSupelec and Université Paris-Saclay located at Gif-sur-Yvette. Dr. Niculescu is a member of the Inria team "DISCO" and he was the head of L2S for a decade (2010-2019). He is author/coauthor of 11 books and of more than 600 scientific papers. His research interests include delay systems, operator theory, and numerical methods in optimization, and their applications to the design of engineering systems. Since 2017, he is the Chair of the IFAC TC "Linear Control Systems" and he served as Associate Editor for several journals in Control area, including the IEEE Transactions on Automatic Control (2003-2005). IEEE Fellow since 2018, he is Doctor Honoris Causa of University of Craiova (Romania) since 2016, Founding Editor and Editor-in-Chief of the Springer Nature Series "Advances in delays and dynamics" since its creation in 2012. For further information, please visit https://cv.archives-ouvertes.fr/silviu-iulian-niculescu